

EUROPEAN ORGANIZATION FOR NUCLEAR RESEARCH  
Proposal to the ISOLDE and Neutron Time-of-Flight Committee

High precision  $^{209}\text{Bi}(n,\gamma)$  cross section measurement at  
n\_TOF EAR2

September 26, 2023

J. Balibrea-Correa<sup>1</sup>, C. Domingo-Pardo<sup>1</sup>, G. de la Fuente<sup>1</sup>, J. Lerendegui-Marco<sup>1</sup>,  
B. Gameiro<sup>1</sup>, A. Tarifeño-Saldivia<sup>1</sup>, V. Babiano-Suárez<sup>2</sup>, F. Calviño<sup>3</sup>, A. Casanovas<sup>3</sup>,  
G. Cortes<sup>3</sup>, V. Alcayne<sup>4</sup>, D. Cano-Ott<sup>4</sup>, T. Martinez<sup>4</sup>, E. Mendoza<sup>4</sup>, A. Pérez-de-Rada<sup>4</sup>,  
A. Sánchez-Caballero<sup>4</sup>, M. Bacak<sup>5</sup>, N. Patronis<sup>5</sup>, A. Wallner<sup>6</sup>  
and the n\_TOF Collaboration<sup>7</sup>

<sup>1</sup> *Instituto de Física Corpuscular, CSIC - Universidad de Valencia, Spain*

<sup>2</sup> *Universitat de València, Spain*

<sup>3</sup> *Universitat Politècnica de Catalunya, Spain*

<sup>4</sup> *Centro de Investigaciones Energéticas, Medioambientales y Tecnológicas (CIEMAT), Spain*

<sup>5</sup> *European Organization for Nuclear Research (CERN), Switzerland*

<sup>6</sup> *Helmholtz-Zentrum Dresden-Rossendorf, Germany*

<sup>7</sup> *www.cern.ch/n\_TOF*

**Spokesperson:** J. Balibrea-Correa (javier.balibrea@ific.uv.es)

**Technical coordinator:** O. Aberle (oliver.aberle@cern.ch)

**Abstract:**

The  $^{209}\text{Bi}(n,\gamma)$  cross section is one of the key elements to estimate the radiological burden associated to  $^{210}\text{Po}$  inventory in innovative lead-bismuth cooled GenIV nuclear reactors and ADS. Additionally,  $^{209}\text{Bi}$  plays a crucial role for the understanding of Th and U chronometers. The current proposal aims to measure the aforementioned cross section in the neutron energy range covering from thermal up to 100 keV with a target accuracy below 10% in the resolved resonance region (<30 keV) and between 20% and 30% up to 100 keV. Through the proposed measurement previous limitations due to small signal to background ratio can be overpassed. This is only possible because of n\_TOF's generation III spallation target, greatly improving the resolution function of EAR2, the use of the high sensitivity sTED array and several optimizations carried out in the last experimental campaigns.

**Requested protons:**  $3 \times 10^{18}$  protons on target

**Experimental Area:** EAR2



# 1 Introduction

New generations of advanced nuclear power plants such as GenIV reactors, Small Modular Reactors (SMR) and Accelerator Driven Systems (ADS) aim to excel safety and reliability during operation, sustainability, minimization of long-term nuclear waste and comply with non proliferation agreements [1]. Microscopic nuclear data plays a key role for those innovative GenIV and SMR nuclear reactors during design optimization, safety margins reduction and improved control of nuclear waste production and inventory. On the other hand, nuclear data is crucial to design innovative ADS systems aiming to produce energy combining MOX nuclear fuel with byproducts from other nuclear reactors, thereby reducing the radiotoxicity of the final nuclear waste.

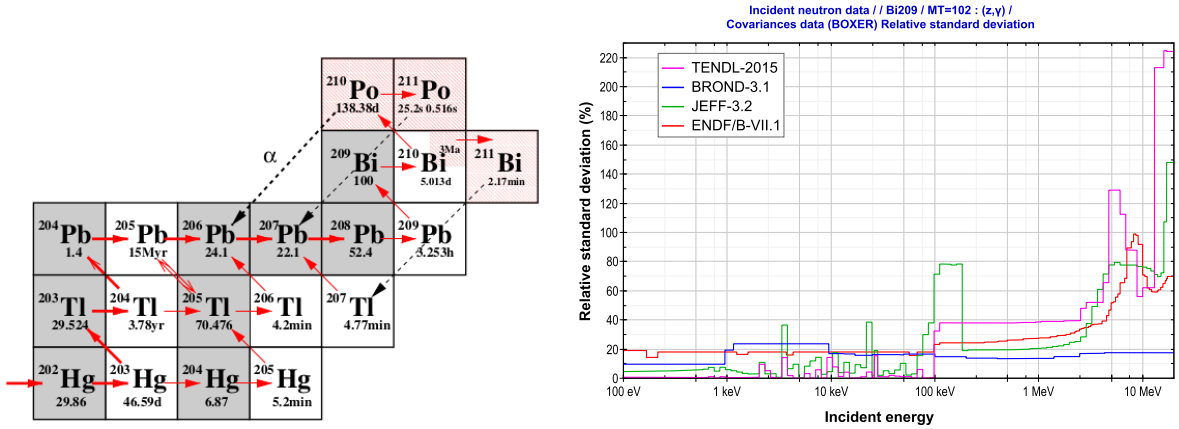


Figure 1: Left: Zoom of the nuclear chart for the lead/bismuth isotope region. Right:  $^{209}\text{Bi}(n,\gamma)$  uncertainty as a function of neutron energy for different evaluated libraries. Figures adapted from references [2] and [3].

MYRRHA (Multi-purpose HYbrid Research Reactor for High-tech Applications) [4] is an experimental ADS cooled by a lead-bismuth mixture. Fast neutrons are produced via spallation reactions using a 600 MeV proton beam. The radiological burden associated with the use of this type of coolant for MYRRHA and other fast nuclear systems is given by the production of  $^{210}\text{Po}$  isotope.  $^{210}\text{Po}$  is a byproduct from  $(n,\gamma)$  reactions on  $^{209}\text{Bi}$  to the ground state that quickly decays to  $^{210}\text{Pb}$  ( $t_{1/2} \sim 5$  days). Additionally, the same reaction can produce a metastable state that can decay to  $^{206}\text{Tl}$  ( $t_{1/2} \sim 3\text{My}$ ). The left panel of Fig 1 shows a zoom of the nuclear chart for lead bismuth isotopes region for illustration of the process. There are significant discrepancies between  $^{209}\text{Bi}(n,\gamma)$  evaluations and the branching to the metastable state, which constitute a severe constraint for the accurate prediction of  $^{210}\text{Po}$  content in lead-bismuth cooled fast nuclear reactor concepts. For instance, the concentration uncertainty of  $^{210}\text{Po}$  after one irradiation cycle of MYRRHA ranges from 5 to 20% depending on the evaluation. This uncertainty does not cover the deviation between calculated and observed concentration values. Therefore, only the accurate knowledge of both reaction channels and its branching ratio can accurately predict the inventory of  $^{210}\text{Po}$  for lead-bismuth heavy coolant nuclear systems. As shown in the right panel of Fig. 1, the  $^{209}\text{Bi}(n,\gamma)$  evaluated cross section uncertainty is large with values ranging between 20% and 40% for neutron resonances up to 100 keV and uncertainties

larger than 80% for neutron energies above 100 keV [3]. Because of the aforementioned reasons,  $^{209}\text{Bi}(n,\gamma)$  and  $^{209m}\text{Bi}(n,\gamma)$  cross sections are included in the OECD's Nuclear Energy Agency (*NEA*) High Priority Request List (HPRL) [5]. In current request, it is stated that significant efforts are needed to reduce discrepancies between evaluations. In particular, new accurate Time of Flight (ToF) data will address  $(n,\gamma)$  uncertainty and incompatibilities between libraries in the region from thermal up to neutron energies of lead-bismuth cooled reactors operation [3, 5]. According to the *NEA*, a future evaluation of this important cross section should be supported by additional accurate experimental data on both,  $^{209}\text{Bi}(n,\gamma)$  and  $^{209m}\text{Bi}(n,\gamma)$  reaction channels. Furthermore,  $^{209}\text{Bi}$  is the last stable isotope in the neutron capture chain of the  $s$ -process reaction path [14, 15]. Neutron capture on  $^{209}\text{Bi}$  populates the isomer as well as the ground state of  $^{210}\text{Bi}$ . At the higher  $s$ -process temperatures, however, the isomeric state  $^{210m}\text{Bi}$  is quickly depopulated to the short lived ground state by the photon bath and, therefore, a more important role is played by the short-lived ground state ( $t_{1/2} = 5.013$  d), which  $\beta$ -decays into the  $\alpha$ -unstable isotope  $^{210}\text{Po}$  ( $t_{1/2} = 138.38$  d). From  $^{210,211}\text{Po}$  starts the main recycling of the  $s$ -process via  $\alpha$ -decay. Improved nuclear physics data are necessary to estimate the accumulation of the  $s$ -process material beyond  $^{206}\text{Pb}$ , and to consolidate the reliability of the Th and U chronometers. An independent measurement to the isomeric state applying a combination of activation and subsequent Accelerator Mass Spectrometry is presently in progress for thermal energies as well as for a quasi-stellar neutron spectrum around 25 keV.

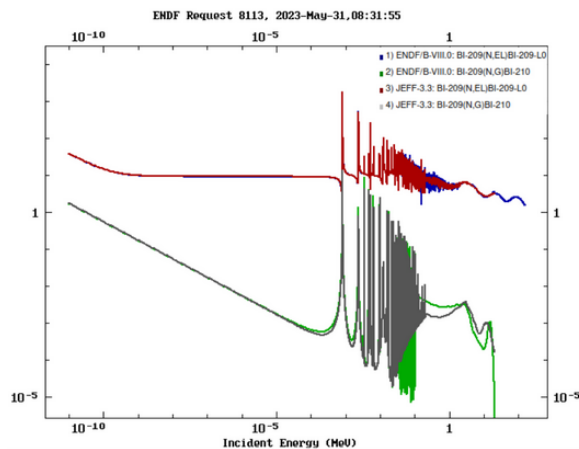


Figure 2:  $^{209}\text{Bi}(n,\gamma)$  and  $^{209}\text{Bi}(n,\text{el})$  cross sections for ENDF/B-VIII.1 and JEFF3.3 evaluated libraries.

However, to measure the  $^{209}\text{Bi}(n,\gamma)$  cross section is challenging because of the small  $(n,\gamma)$  cross section and large  $(n,\text{el})$  to  $(n,\gamma)$  reaction channels as shown in Fig. 2. The most recent  $^{209}\text{Bi}(n,\gamma)$  ToF measurement was performed at CERN n\_TOF EAR1 by *C. Domingo* and collaborators in 2006 using the state-of-the-art low neutron sensitivity  $\text{C}_6\text{D}_6$  detectors [2]. However the target uncertainty could not be reached due to a significant in-beam  $\gamma$ -ray background and insufficient EAR1 luminosity. Those conditions have been significantly improved with the high luminosity EAR2 and refined spallation source design [6, 7, 8]. Recently, in combination with the high sensitivity sTED [9] array detection setup, EAR2

has demonstrated its potential for challenging  $(n,\gamma)$  cross section measurements in a broad neutron energy range [10, 11, 12, 13].

## 2 Proposed experiment

The goal of the present proposal is the  $^{209}\text{Bi}(n,\gamma)$  cross section measurement at EAR2 with an statistical accuracy for resonance kernels (integrals) better than 10% in the neutron energy range covering thermal up to 30 keV. For higher energies, the  $(n,\gamma)$  cross-section will be estimated as unresolved resonance region up to a minimum neutron energy of 100 keV paying special attention to systematics related to self-shielding, multiple scattering, background estimation and normalization. The overall uncertainty in the latter is expected not be larger than 20%. The estimated resolved region is based on the results from a previous experimental campaign in which the first  $^{209}\text{Bi}(n,\gamma)$  resonance was used for detectors optimization (See Fig. 7 in Appendix A).

### 2.1 Experimental setup and targets

In order to overcome previous limitations and achieve the target uncertainty required for a new evaluation [5], we will use the compact, high sensitivity, sTED detector array in a configuration similar to the one used for  $^{94}\text{Nb}(n,\gamma)$  and  $^{79}\text{Se}(n,\gamma)$  measurements performed in 2022 [10, 12]. Two conventional  $\text{C}_6\text{D}_6$  will be placed together with the sTED array to reduce possible systematics associated to anisotropies or presence of angular distributions. A picture of the experimental setup used for  $(n,\gamma)$  campaign in 2022 is shown in Fig. 3.

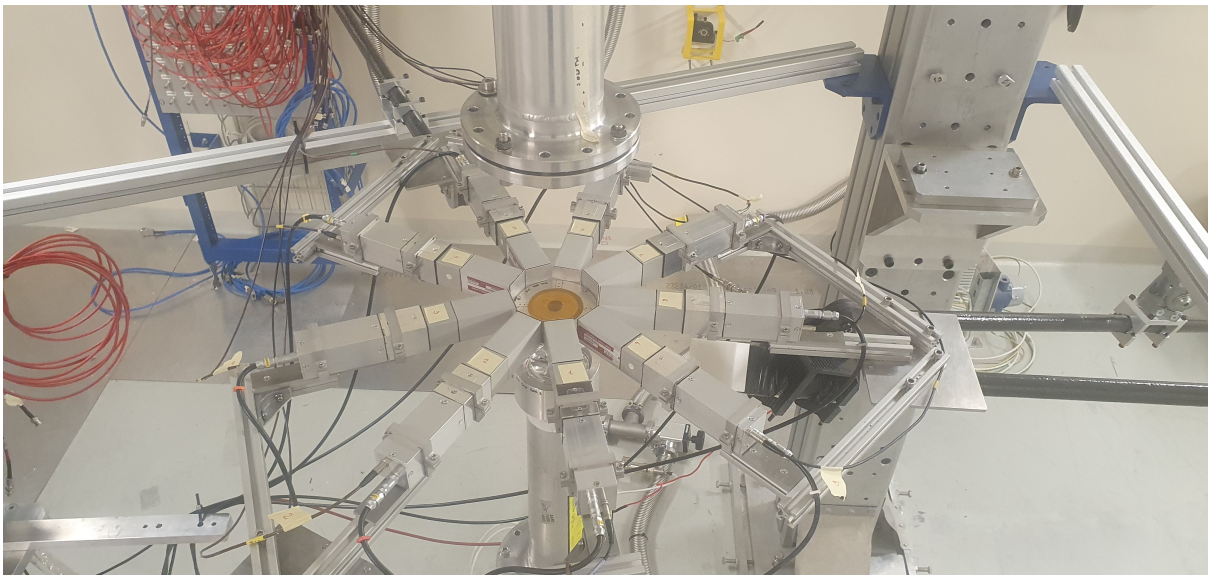


Figure 3: State-of-the-art sTED array and  $\text{C}_6\text{D}_6$  detectors placed in EAR2 during the  $^{94}\text{Nb}(n,\gamma)$  and  $^{79}\text{Se}(n,\gamma)$  experiments in 2022.

The efficiency of the proposed setup for  $^{209}\text{Bi}(n,\gamma)$  reaction was estimated using Monte Carlo (MC) simulations. First, realistic  $(n,\gamma)$  cascades were generated using the NUDEX

decay generator [16], using default parameters for photon strength functions and level density. Then, the  $\gamma$ -ray cascades were transported into a detailed geometry implemented in a C++ application based on the GEANT4 toolkit. The efficiency for the sTED array and the two  $C_6D_6$  detectors, using an individual detection threshold of 200 keV, is 4.6% and 2.1%, respectively. We propose the use of two hyper-pure  $^{209}\text{Bi}$  targets of 21 mm diameter and different thickness, 1 and 6 mm. The combination of the data from the two targets is expected to achieve target uncertainty determining the resonance parameters while reducing systematics from multiple scattering and self-shielding corrections effects [17]. In the rest of the proposal both thicknesses will be labelled as *thin* and *thick* targets. High purity  $^{209}\text{Bi}$  material (>99%) is already [available](#) in metallic form with several thickness suitable for  $(n,\gamma)$  ToF measurements and compatible with the current proposal.

## 2.2 Expected results and requested protons

The JEFF3.3 evaluated  $^{209}\text{Bi}(n,\gamma)$  cross section was used for a count rate estimation of *thin* and *thick* configurations. Multiple scattering, self-shielding and EAR2 Resolution function were included in the calculation using the SAMMY code. The cross section was convoluted with EAR2 neutron fluence and scaled properly using the calculated detection efficiency. The expected  $^{209}\text{Bi}(n,\gamma)$  reaction yield per high intensity proton pulse (3000 bins/decade) using *thin* and *thick* targets are displayed by the black lines in left and right panels of Fig. 4.

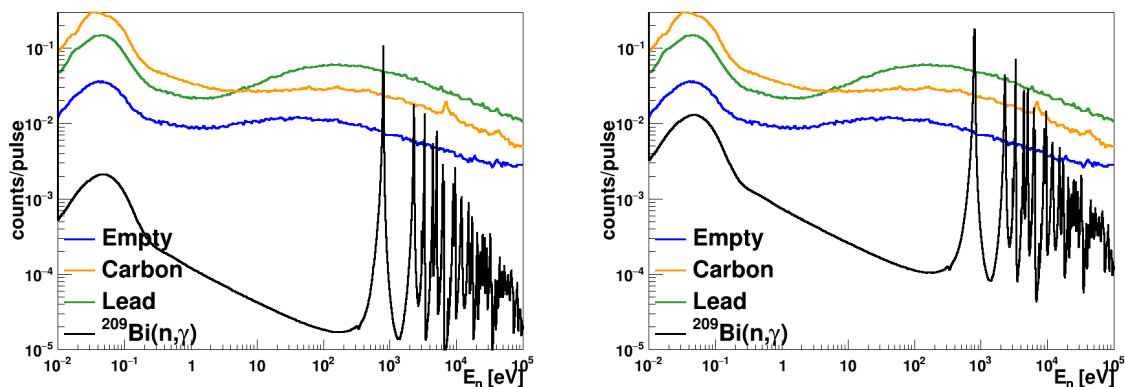


Figure 4: Expected  $^{209}\text{Bi}(n,\gamma)$  number of counts per pulse (black) together with experimental background measurements: Empty (blue), C (orange), Lead (green). Left: *thin* target. Right: *thick* target.

In the same plot are presented experimental average number of counts per high intensity pulse for Empty, Carbon and Lead configurations usually devoted to background estimation. As in previous proposals, MC experiments were performed to optimize the number of protons devoted to each individual configuration, simulating in the process background subtraction for the calculated reaction yield. Description and further information about this process can be found in [10, 12]. After an optimization process attending to the results from MC simulations, the optimal proton distribution for the different configurations is summarized in Tab. 1. The Background configuration is comprised of several

measurements, i.e. no sample and also Carbon and Lead samples to estimate the neutron scattering and in-beam  $\gamma$ -ray contributions to the background respectively.

Configuration	Protons [ $10^{18}$ ]
<i>Thick target</i>	0.8
<i>Thin target</i>	0.8
Background	1.2
Normalization	0.2
<b>Total</b>	<b>3.0</b>

Table 1: Summary of requested number of protons for the individual configurations in the current proposal. At last, the total requested protons is summarized.

*Thin* and *thick* total yield were calculated combining lead background and  $^{209}\text{Bi}(n,\gamma)$  counts per pulse shown in Fig. 4. Then, the reaction yield is calculated as the difference between both configurations. The MC background subtracted results for *thick* and *thin* targets at the two first resonances are shown in both panels of Fig. 5. Together with the MC reaction yield is shown the JEFF.3.3  $^{209}\text{Bi}(n,\gamma)$  including multiple scattering, self-shielding and resolution function effects. As shown in Fig. 5, the resonances for *thin* and *thick* configurations are well defined but quite different because of the self-shielding and multiple scattering effects. Thus, combining both datasets, the corrections can be properly addressed as demonstrated in [17]. The same calculation, but for all individual resonances up to 30 keV is displayed in Fig. 8 of appendix B.

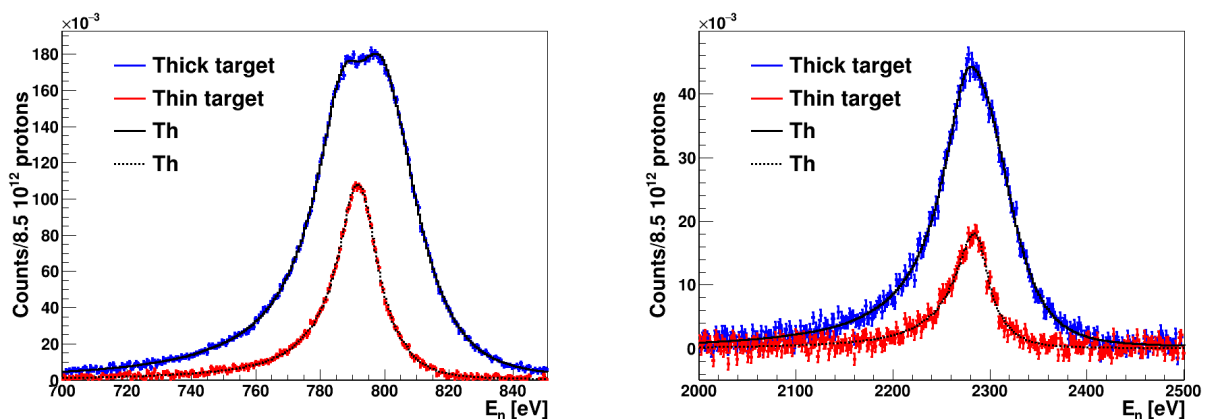


Figure 5: MC  $^{209}\text{Bi}(n,\gamma)$  (3000 bins/decade) yield for thick and thin target in the two first neutron resonances. In the same plot is included the JEFF3.3 evaluated cross section including multiple scattering, self-shielding effects and resolution function using SAMMY.

Fig. 6 shows the expected statistical uncertainty in the resonance kernel (integral) for *thick* and *thin* configurations as a function of the neutron energy. In average, the expected statistical uncertainty for the goal resolved resonance region range ( $<30$  keV) is 5% while in the last expected resonances the statistical uncertainty is 10% for the *thin* target. It is important to remark that the statistical uncertainty of resonances kernels

is closely related to the uncertainty determining the resonances parameters and systematics associated to multiple scattering and self-shielding as stated before. Thereby, from the measurement and posterior analysis it is expected to fulfill the target uncertainty ( $<10\%$ ) with a systematic uncertainty below 3%, mainly related to multiple scattering and self-shielding for all neutron resonances up to 30 keV.

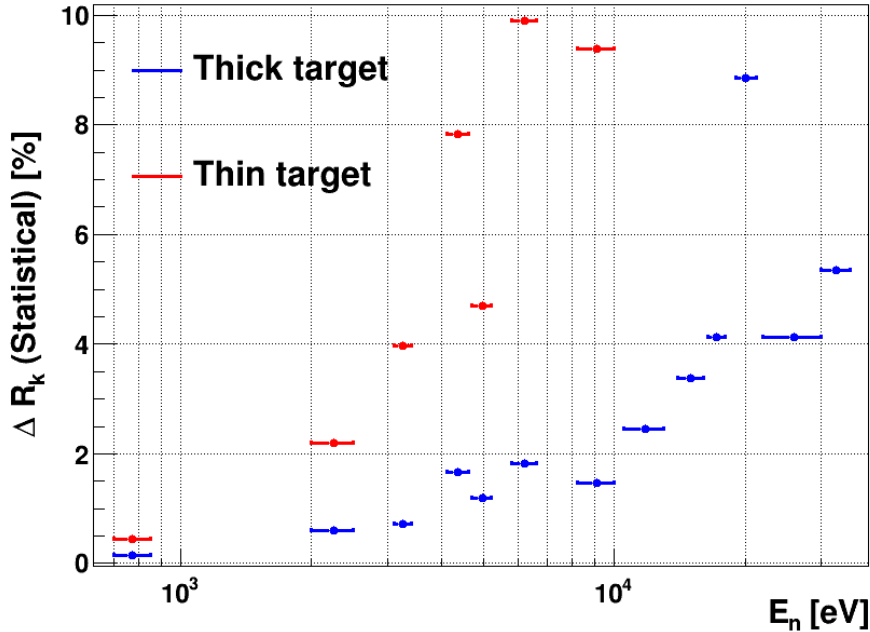


Figure 6: Expected statistical uncertainty, after background subtraction, for individual  $^{209}\text{Bi}(n,\gamma)$  resonances up to neutron energies of 30 keV.

Regarding the non-resolved region, special attention will be paid to systematics uncertainties related to background subtraction. Assuming 1% of systematics and a signal to background ratio of 0.8, the expected maximum uncertainty in the region is 30%. In order to cross-check and validate the results, an independent cross section calculation will be performed using a Hauser-Feshbach formalism.

As an outlook, we are planning to complement this ToF proposal with a future proposal for an activation measurement at NEAR to accurately determine the  $^{209m}\text{Bi}(n,\gamma)/^{209}\text{Bi}(n,\gamma)$  contribution to the different neutron resonances. This is only possible because of the half life of  $^{210}\text{Po}$  ( $t_{1/2} \sim 5$  years) and the large versatility of NEAR to mimic different neutron energy spectras.

**Summary of requested protons:**  $3 \times 10^{18}$  .

## References

- [1] GenIV International Forum.
- [2] C. Domingo-Pardo et al. *Physical Review C*, **74** 025807.
- [3] L. Fiorito et al. *EPJ Nuclear Sci. Technol.* (2018) **4**, 48.
- [4] Multi-purpose HYbrid Research Reactor for High-tech Applications.
- [5] High Priority Request List:  $^{209}\text{Bi}(n,\gamma)$ .
- [6] R. Esposito et al. *Phys. Rev. Accel. Beams* (2021) **24**, 093001.
- [7] N. Patronis et al. *EPJ Techniques and Instrumentation* (2023) **10**, 13.
- [8] J. Leredegui et al. *15th EPJ Web of Conferences* (2023), **284**, 01028.
- [9] V. Alcayne et al. *15th EPJ Web of Conferences* (2023), **284**, 01043.
- [10] First measurement of the  $^{94}\text{Nb}(n,\gamma)$  cross-section (2020)
- [11] J. Balibrea-Correa et al. *EPJ Web of Conferences* (2023) **279**, 06004.
- [12] First measurement of the s-process branching  $^{79}\text{Se}(n,\gamma)$  (2020)
- [13] J. Leredegui et al. *EPJ Web of Conferences* (2023) **279**, 13001.
- [14] C. Travaglio, D. Galli, R. Gallino, M. Busso, F. Ferrini, and O. Straniero, *Astrophys. J.* **521**, 691 (1999).
- [15] C. Travaglio, R. Gallino, M. Busso, and R. Gratton, *Astrophys. J.* **549**, 346 (2001).
- [16] E. Mendoza et al. *Nuclear Instruments and Method A* (2023) **1047**, 167894.
- [17] A. Kimura *Journal of Nuclear Science and Technology* **56:6**, 479 (2019)



# Appendix

## DESCRIPTION OF THE PROPOSED EXPERIMENT

Please describe here below the main parts of your experimental set-up:

Part of the experiment	Design and manufacturing
If relevant, write here the name of the <u>fixed</u> installation you will be using sTED present in n_TOF EAR2	<input checked="" type="checkbox"/> To be used without any modification <input type="checkbox"/> To be modified
If relevant, describe here the name of the flexible/transported equipment you will bring to CERN from your Institute [Part 1 of experiment/ equipment]	<input type="checkbox"/> Standard equipment supplied by a manufacturer <input type="checkbox"/> CERN/collaboration responsible for the design and/or manufacturing
[Part 2 of experiment/ equipment]	<input type="checkbox"/> Standard equipment supplied by a manufacturer <input type="checkbox"/> CERN/collaboration responsible for the design and/or manufacturing
[insert lines if needed]	

## HAZARDS GENERATED BY THE EXPERIMENT

Additional hazard from flexible or transported equipment to the CERN site:

Domain	Hazards/Hazardous Activities	Description
Mechanical Safety	Pressure	<input type="checkbox"/> [pressure] [bar], [volume][l]
	Vacuum	<input type="checkbox"/>
	Machine tools	<input type="checkbox"/>
	Mechanical energy (moving parts)	<input type="checkbox"/>
	Hot/Cold surfaces	<input type="checkbox"/>
Cryogenic Safety	Cryogenic fluid	<input type="checkbox"/> [fluid] [m3]
Electrical Safety	Electrical equipment and installations	<input type="checkbox"/> [voltage] [V], [current] [A]
	High Voltage equipment	<input type="checkbox"/> <a href="https://myrrha.be/">https://myrrha.be/</a> [voltage] [V]
Chemical Safety	CMR (carcinogens, mutagens and toxic to reproduction)	<input type="checkbox"/> [fluid], [quantity]
	Toxic/Irritant	<input type="checkbox"/> [fluid], [quantity]
	Corrosive	<input type="checkbox"/> [fluid], [quantity]
	Oxidizing	<input type="checkbox"/> [fluid], [quantity]
	Flammable/Potentially explosive atmospheres	<input type="checkbox"/> [fluid], [quantity]
	Dangerous for the environment	<input type="checkbox"/> [fluid], [quantity]
Non-ionizing radiation Safety	Laser	<input type="checkbox"/> [laser], [class]
	UV light	<input type="checkbox"/>
	Magnetic field	<input type="checkbox"/> [magnetic field] [T]

Workplace	Excessive noise	<input type="checkbox"/>	
	Working outside normal working hours	<input type="checkbox"/>	
	Working at height (climbing platforms, etc.)	<input type="checkbox"/>	
	Outdoor activities	<input type="checkbox"/>	
Fire Safety	Ignition sources	<input type="checkbox"/>	
	Combustible Materials	<input type="checkbox"/>	
	Hot Work (e.g. welding, grinding)	<input type="checkbox"/>	
Other hazards			

## Appendix A

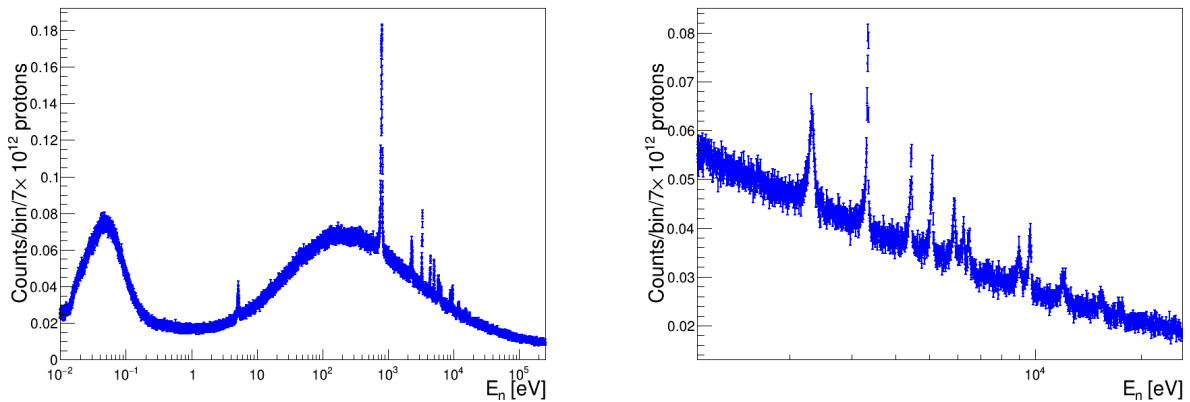


Figure 7: Experimental  $^{209}\text{Bi}(n,\gamma)$  reaction yield measured using 3 sTED individual detectors and  $7.5 \times 10^{17}$  protons on target during the last optimization campaign.

# Appendix B

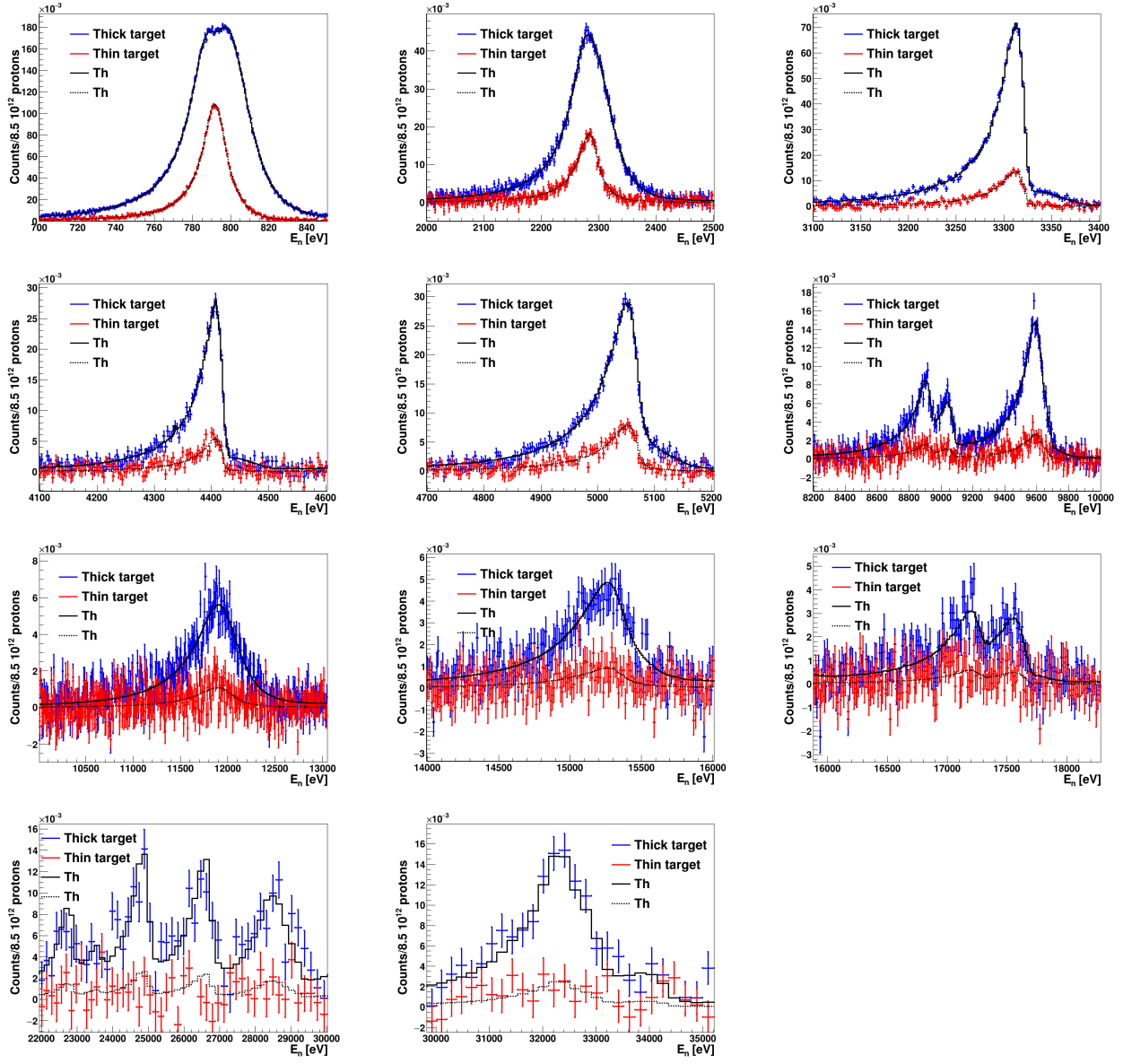


Figure 8: MC  $^{209}\text{Bi}(n,\gamma)$  reaction yield estimated for *thin* and *thick* configurations in the individual neutron resonances up to 30 keV included in the evaluated library JEFF 3.3.